Systematic study of α decay half-lives of doubly odd nuclei within the two-potential approach

Xiao-Dong Sun,[1] Jun-Gang Deng,[2] Dong Xiang,[2,*] Ping Guo,[1] and Xiao-Hua Li[2,3,4,†]

[1]*School of Math and Physics, University of South China, 421001 Hengyang, People's Republic of China*

[2]*School of Nuclear Science and Technology, University of South China, 421001 Hengyang, People's Republic of China*

[3]*Cooperative Innovation Center for Nuclear Fuel Cycle Technology & Equipment, University of South China, 421001 Hengyang, People's Republic of China*

[4]*Key Laboratory of Low Dimensional Quantum Structures and Quantum Control, Hunan Normal University, 410081 Changsha, People's Republic of China*

(Received 22 January 2017; published 3 April 2017)

α decay is a common and important process of natural radioactivity of the heavy and superheavy nuclei. From the α decay of nuclei, we can obtain much more information of nuclei structure. In our previous works [X.-D. Sun *et al.*, Phys. Rev. C **93**, 034316 (2016); X.-D. Sun *et al.*, *ibid.* **95**, 014319 (2017)], we have done systematic study on the α preformation probability of both the even-even and odd-A nuclei within the two-potential approach. The α preformation probabilities will systematically change due to the shell effect, proton-neutron correlation, and so on. This work is the extension of the previous works. In this work, we systematically study the α decay of doubly odd nuclei. We find that for superallowed α decay the α preformation probabilities of doubly odd nuclei are larger than those of odd-A ones in general, and for the heavier nuclei the extra neutrons suppress the proton-neutron correlation resulting in the small α preformation probabilities. The calculated results can well reproduce the experimental half-lives. The half-lives of the α decay chain beginning from nuclide $^{296}119$ are also predicted and compared with various empirical formulas.

DOI: 10.1103/PhysRevC.95.044303

I. INTRODUCTION

Since α decay was defined in 1899 by Rutherford, great efforts have been made in the realm of both theory and experiment, e.g., from the discovery of the atomic nucleus by α particle scattering to the Geiger-Nuttall law depicting a relation between α decay half-life and decay energy [1–5], from the barrier tunneling theory according to the quantum mechanics to the investigation of proton-rich and superheavy nuclei [6–13]. Up to now nearly 600 α radioactivity nuclei or isomers have been detected and measured, including over 140 doubly odd nuclei [14,15]. In the case of doubly odd nuclei, the unpaired proton and neutron present some interesting results. On the one hand, an island of light α radioactivity nuclei appears above the exotic doubly magic nucleus ^{100}Sn, the heaviest $N = Z$ nucleus, where both proton and neutron move in the same shell and the enhanced correlation arises between neutron and proton. Thus, these nuclei are known as superallowed α decay with large α particle preformation probability [16–20]. Moreover, the Pauli blocking effect coming from both the unpaired proton and neutron is weakened, resulting in the increase of α preformation probability of doubly odd nuclei compared with the neighboring odd-A nuclei. Besides, it has been found that the α decay nucleus ^{108}I locates beyond the proton drop line [20]. On the other hand, the total hindrance factor produced by odd proton and neutron significantly prolongs fission lifetimes for the superheavy nuclei [12,21]. Therefore α decay chains from the new synthesized doubly odd nuclei $^{294}_{117}$Ts are extremely long and end at dubnium ^{270}Db by spontaneous fission [12].

Following the Gamow theory, α decay is interpreted as the classical two-step mechanism with quantum tunneling effect [6,22]. In 1966, the Viola-Seaborg formula took into account the even-odd stagger of α decay half-lives by introducing hindrance factor h [4,5]. Afterwards α decay was considered to be a very asymmetric fission process [23], and the α preformation probability is interpreted as the penetrability of the prescission part of the barrier [24]. The quasimolecular shape mechanism is also introduced to describe the nuclear shape evolution based on the liquid drop model [25,26]. As a result of nuclear shell structure, α emitters below and above $N = 126$ shell closure follow the different quantum numbers of α-core relative motion, implying α cluster structure in nuclei [27]. Over time, more and more nuclear structure effects are considered in α decay, and the α cluster structure is interesting and worthy of investigation [28–34]. The α cluster preformation probability can be extracted from the experimental α decay half-lives, and analyzed based on the shell effect and various residual interactions, such as the pairing force as well as proton-neutron correlation and so on [33,35–40]. Meanwhile, the microscopic calculations about α cluster structure, e.g., the shell model [41,42] and quarteting wave function [43], are still improving. In addition, the competition among α decay, proton emission, cluster radioactivity, and spontaneous fission is crucial to stability of the heavy and superheavy nuclei [44–51]. Previously, we systematically studied the α decay half-lives of both even-even and odd-A nuclei by using the isospin-dependent nuclear potential, whose parameters are obtained by fitting the α decay half-lives of even-even nuclei because the influence coming from the unfavored decay can be neglected [52]. The

*xiangdong007@163.com

†lixiaohuaphysics@126.com

α preformation probabilities are analyzed taking into account the nuclear shell effect utilizing an analytic formula. The calculated results can well reproduce the experimental α decay half-lives [52]. So it is necessary to test the validity of the method for doubly odd nuclei and to study systematically the α decay properties of the heavy and superheavy nuclei. This constitutes the motivation of this work.

This article is organized as follows. In Sec. II, the theoretical framework for the calculation of the α decay half-lives is briefly described. In Sec. III, we show the systematic results of α decay half-lives for doubly odd nuclei, especially for superallowed α decay and superheavy nuclei. The calculated α decay half-lives and the estimated α preformation probabilities are given and discussed. A brief summary is given in Sec. IV.

II. THEORETICAL FRAMEWORK

The two-potential approach was proposed by Gurvitz and Kalbermann to treat the decay of a quasistationary state that bridges the bound and scattering states [53]. In the two-potential approach, the Gamow formula is improved by adding a well-defined preexponential factor. Then, the decay width Γ can be written as

$$\Gamma = P_0 P_\alpha F \frac{\hbar^2}{4\mu} \exp\left[-2\int_{r_2}^{r_3} k(r)dr\right], \tag{1}$$

where P_α, F denote the α preformation probability, normalized factor, respectively. The part of exponential function expresses the barrier tunneling similar to the Gamow formula. The preformation factor P_0 is introduced to provide the average α preformation probability of one certain kind of α decay nuclei, i.e., $P_0 = 0.43$ for even-even nuclei, $P_0 = 0.35$ for odd-A nuclei, $P_0 = 0.18$ for doubly odd nuclei [54]. The normalized factor F, expressing the assault frequency, can be approximated as

$$F\int_{r_1}^{r_2} \frac{dr}{2k(r)} = 1, \tag{2}$$

where $k(r) = \sqrt{\frac{2\mu}{\hbar^2} \mid Q_\alpha - V(r) \mid}$ is the wave number. The μ denotes the reduced mass of the α particle and daughter nucleus. The r indicates the mass center distance between the preformed α particle and the daughter nucleus. In detail, the r_1, r_2, and r_3 are the classical inner, middle, and outer turning points, respectively. They must satisfy the conditions $V(r_1) = V(r_2) = V(r_3) = Q_\alpha$. The α decay half-life is

$$T_{1/2} = \frac{\hbar \ln 2}{\Gamma}. \tag{3}$$

The potential between the preformed α particle and the daughter nucleus, including the nuclear, Coulomb, and centrifugal potential barrier, can be written as

$$V(r) = V_{\rm N}(r) + V_{\rm C}(r) + V_{\rm l}(r), \tag{4}$$

where $V_{\rm N}(r)$ represents the nuclear potential. In this work, we choose a type of cosh for the nuclear potential [55]. It can be expressed as

$$V_{\rm N}(r) = -V_0 \frac{1+\cosh(R/a)}{\cosh(r/a)+\cosh(R/a)}, \tag{5}$$

where V_0 and a are the depth and diffuseness of the nuclear potential, respectively. In our previous work [52] through analyzing the experimental α decay half-lives of 164 even-even nuclei, we have obtained a set of isospin-dependent nuclear potential parameters, i.e., $a = 0.5958$ fm, $V_0 = 192.42 + 31.059\frac{N_{\rm d}-Z_{\rm d}}{A_{\rm d}}$ MeV, where $N_{\rm d}$, $Z_{\rm d}$, and $A_{\rm d}$ denote the neutron, proton, and mass number of the daughter nucleus, respectively. $V_{\rm C}(r)$ is the Coulomb potential and is taken as the potential of a uniformly charged sphere with sharp radius R, which can be expressed as

$$V_{\rm C}(r) = \begin{cases} \frac{Z_{\rm d} Z_\alpha e^2}{2R}\left[3 - \left(\frac{r}{R}\right)^2\right], & r < R \\ \frac{Z_{\rm d} Z_\alpha e^2}{r}, & r > R, \end{cases} \tag{6}$$

where Z_α is the proton number of the α particle. The sharp radius R is given by

$$R = 1.28A^{1/3} - 0.76 + 0.8A^{-1/3}. \tag{7}$$

This empirical formula, which is derived from the nuclear droplet model and the proximity energy, is commonly used to calculate α decay half-lives [56]. The last part, langer-modified centrifugal potential, can be estimated by

$$V_{\rm l}(r) = \frac{\hbar^2}{2\mu r^2}\left(l + \frac{1}{2}\right)^2, \tag{8}$$

where l is the orbital angular momentum taken away by α particle.

The α preformation probability can be extracted from the experimental α decay half-lives [31,35,37]. If $P_\alpha = 1$ and $P_0 = 1$, the calculated α decay half-lives are defined as $T_{1/2,\alpha}^{\rm calc1}$. We can use $T_{1/2,\alpha}^{\rm calc1}$ to compare the α preformation probability of different kind of α decay nuclei, i.e., even-even, odd-A, and doubly odd nuclei. In the case of taking into account the preformation factor P_0 only, the calculated α decay half-lives are called as $T_{1/2,\alpha}^{\rm calc2}$. Then the α preformation probability P_α can be extracted by using

$$P_\alpha = \frac{T_{1/2,\alpha}^{\rm calc2}}{T_{1/2,\alpha}^{\rm exp}}. \tag{9}$$

Based on the nuclear shell structure and proton-neutron correlation, the trend of α preformation probabilities can be approximated [26,35,52] by

$$\log_{10} P_\alpha = a + b(Z - Z_1)(Z_2 - Z) + c(N - N_1)(N_2 - N) + dA + e(Z - Z_1)(N - N_1), \tag{10}$$

where Z, N, and A are the proton, neutron, and mass numbers of the α decay parent nucleus. Z_1 and Z_2 (N_1 and N_2) are the proton (neutron) magic numbers around Z (N). a, b, c, d, and e are the adjustable parameters. In the regions with the well-known shell closures, this formula can systematically reproduce the trend of the real α cluster preformation probability in nuclei to some extent. With the estimated α preformation probabilities P_α, the calculated α decay half-lives $T_{1/2,\alpha}^{\rm calc3}$ can be obtained.

TABLE I. Calculation results of α decay half-lives $T_{1/2,\alpha}^{\mathrm{calc1}}$ including even-even, odd-A, and doubly odd nuclei in the superallowed α decay island above the exotic doubly magic nucleus ^{100}Sn.

α transition	I_i^π	I_j^π	l_{min}	Q_α(MeV)	$T_{1/2,\alpha}^{\mathrm{exp}}$(s)	$T_{1/2,\alpha}^{\mathrm{calc1}}$(s)	$T_{1/2,\alpha}^{\mathrm{calc1}}/T_{1/2,\alpha}^{\mathrm{exp}}$
^{105}Te → ^{101}Sn	(7/2$^+$)	(7/2$^+$)	0	5.075	6.33×10^{-7}	3.88×10^{-8}	0.061
^{106}Te → ^{102}Sn	0$^+$	0$^+$	0	4.285	8×10^{-5}	5.44×10^{-5}	0.68
^{107}Te → ^{103}Sn	5/2$^+$#	5/2$^+$#	0	4.005	4.43×10^{-3}	1.16×10^{-3}	0.261
^{108}Te → ^{104}Sn	0$^+$	0$^+$	0	3.420	4.29×10^{0}	2.53×10^{0}	0.591
^{109}Te → ^{105}Sn	(5/2$^+$)	(5/2$^+$)	0	3.198	1.18×10^{2}	7.9×10^{1}	0.669
^{110}Te → ^{106}Sn	0$^+$	0$^+$	0	2.699	6.2×10^{5}	9.28×10^{5}	1.496
^{108}I → ^{104}Sb	1$^+$#	–	0	4.099	3.96×10^{-2}	1.5×10^{-3}	0.038
^{109}I → ^{105}Sb	1/2$^+$	(5/2$^+$)	2	3.918	7.36×10^{-1}	2.86×10^{-2}	0.039
^{110}I → ^{106}Sb	(1$^+$)	(2$^+$)	2	3.588	3.91×10^{0}	2.15×10^{0}	0.55
^{111}I → ^{107}Sb	5/2$^+$#	5/2$^+$#	0	3.274	$\sim 2.5 \times 10^{3}$	1.04×10^{2}	0.041
^{112}I → ^{108}Sb	1$^+$#	(4$^+$)	4	2.957	2.85×10^{5}	4.62×10^{5}	1.619
^{113}I → ^{109}Sb	5/2$^+$#	5/2$^+$#	0	2.706	1.99×10^{9}	4.24×10^{6}	0.002
^{109}Xe → ^{105}Te	7/2$^+$#	(7/2$^+$)	0	4.215	1.3×10^{-2}	1.5×10^{-3}	0.115
^{110}Xe → ^{106}Te	0$^+$	0$^+$	0	3.875	1.45×10^{-1}	8.52×10^{-2}	0.587
^{111}Xe → ^{107}Te	5/2$^+$#	5/2$^+$#	0	3.725	7.12×10^{0}	5.86×10^{-1}	0.082
^{112}Xe → ^{108}Te	0$^+$	0$^+$	0	3.331	3×10^{2}	1.96×10^{2}	0.655
^{113}Xe → ^{109}Te	5/2$^+$#	(5/2$^+$)	0	3.086	$\sim 2.49 \times 10^{4}$	1.26×10^{4}	0.507
^{115}Xe → ^{111}Te	(5/2$^+$)	(5/2)$^+$	0	2.505	6×10^{6}	2.82×10^{9}	469.197
^{112}Cs → ^{108}I	1$^+$#	1$^+$#	0	3.935	$>1.88 \times 10^{-1}$	1.51×10^{-1}	0.799
^{114}Cs → ^{110}I	(1$^+$)	(1$^+$)	0	3.355	3.17×10^{3}	5.93×10^{2}	0.187
^{114}Ba → ^{110}Xe	0$^+$	0$^+$	0	3.535	5.89×10^{1}	1.68×10^{2}	2.848

III. RESULTS AND DISCUSSIONS

We initially pay attention to the superallowed α decay island. It is well known that as the number of nucleons increases up to $A > 140$, α decay gradually becomes common. The nuclei with light mass are stable against α decay, except the superallowed α decay island above the exotic doubly magic nucleus ^{100}Sn. First, the α decay energy takes local maximum at the position of nuclear magic number plus another two nucleons due to the shell effect [52]. Thus, the proton-rich Te, I, Xe, and Cs isotopes are energy allowed with the α decay energy near 4 MeV. Second, for the $N \sim Z$ nuclei, the α decay occurs prior to proton emission [19]. By contrast, the $A \sim 140$ and $N > Z$ odd-Z isotopes close to the proton drip line, for example, light mass Tm, Ho, and Tb isotopes, undergo proton emission but not α decay. As a result of the strong proton-neutron correlation and the large α preformation probability, this α decay are called the superallowed α decay. The superallowed α decay nuclei are listed in Table I. The first five columns include basic α decay data, such as α transition, spin and parity state of the parent and daughter nuclei, the minimum orbital angular momentum taken away by α particle, and α decay energy, respectively. The experimental data are taken from the NUBASE2012 table [14], and the NNDC web site [15], where "()", "#" indicate uncertain spin and parity, values estimated from trends in around nuclei, respectively. The angular momentum l is obtained under the selection rule according to the spin and parity of both the parent and daughter nuclei [57]. In some cases where the spin and

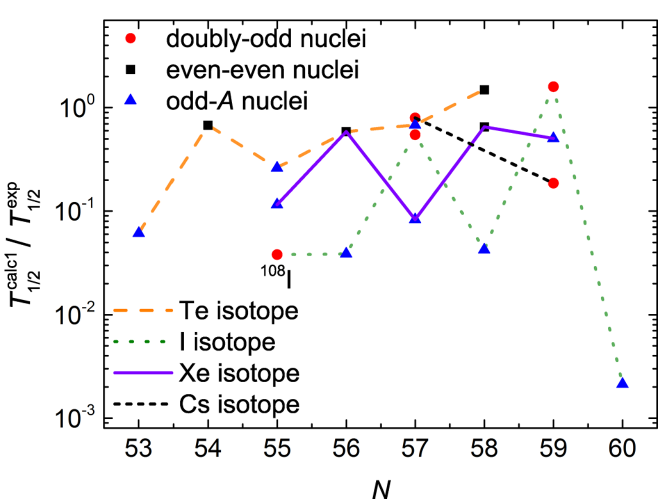

FIG. 1. The ratios of calculated half-lives $T_{1/2,\alpha}^{\mathrm{calc1}}$ to experimental data for the superallowed α decay nuclei as a function of the neutron numbers of the parent nuclei. The tellurium, iodine, xenon, and caesium isotopes are denoted by dashed orange, dotted green, solid violet, and short dashed black lines, respectively.

TABLE II. The parameters to the α preformation probability P_α in Eq. (10) for doubly odd nuclei in four regions.

Reg.	a	b	c	d	e
I	−8.8466	0.0021	0.0006	0.0548	−0.0043
II	−21.3225	0.0009	0.0053	0.0932	0.0019
III	−51.866	−0.0047	−0.0077	0.245	−0.0179
IV	12.397	0.0034	−0.0027	−0.0597	0.0047

TABLE III. Calculation results of α decay half-lives for doubly odd nuclei in four regions within a two-potential approach.

α transition	I_i^π	I_j^π	l_{min}	Q_α(MeV)	$T_{1/2,\alpha}^{exp}$(s)	$T_{1/2,\alpha}^{calc3}$(s)	P_0P_α
				region I			
^{148}Eu → ^{144}Pm	5^-	5^-	0	2.692	5.01×10^{14}	1.22×10^{15}	0.087
^{152}Ho → ^{148}Tb	2^-	2^-	0	4.507	1.35×10^{3}	1.37×10^{3}	0.132
^{152}Ho → ^{148}Tb^m	9^+	$(9)^+$	0	4.577	4.63×10^{2}	5.61×10^{2}	0.132
^{154}Ho → ^{150}Tb	2^-	(2^-)	0	4.042	3.71×10^{6}	8.14×10^{5}	0.134
^{154}Tm → ^{150}Ho	(2^-)	2^-	0	5.094	1.5×10^{1}	1.32×10^{1}	0.155
^{154}Tm^m → ^{150}Ho^m	(9^+)	$(9)^+$	0	5.175	5.69×10^{0}	5.49×10^{0}	0.155
^{156}Tm → ^{152}Ho	2^-	2^-	0	4.345	1.31×10^{5}	1.35×10^{5}	0.151
^{156}Lu^m → ^{152}Tm^m	$(9)^+$	$(9)^+$	0	5.705	2.11×10^{-1}	2.29×10^{-1}	0.174
^{158}Ta → ^{154}Lu	(2^-)	(2^-)	0	6.125	5.1×10^{-2}	3.98×10^{-2}	0.188
^{158}Ta^m → ^{154}Lu^m	(9^+)	(9^+)	0	6.205	3.79×10^{-2}	1.99×10^{-2}	0.188
^{160}Re → ^{156}Ta	(4^-)	(2^-)	2	6.695	5.55×10^{-3}	5.03×10^{-3}	0.196
^{162}Re → ^{158}Ta	(2^-)	(2^-)	0	6.245	1.14×10^{-1}	1.14×10^{-1}	0.17
^{162}Re^m → ^{158}Ta^m	(9^+)	(9^+)	0	6.275	8.46×10^{-2}	8.73×10^{-2}	0.17
^{164}Re^m → ^{160}Ta^m	(9^+)	$(9)^+$	0	5.755	2.97×10^{1}	1.15×10^{1}	0.145
^{166}Re → ^{162}Ta	(7^+)	7^+#	0	5.465	4.5×10^{1}	2.46×10^{2}	0.123
^{166}Ir → ^{162}Re	(2^-)	(2^-)	0	6.725	1.13×10^{-2}	1.75×10^{-2}	0.135
^{166}Ir^m → ^{162}Re^m	(9^+)	(9^+)	0	6.725	1.54×10^{-2}	1.75×10^{-2}	0.135
^{168}Re → ^{164}Ta	(7^+)	(3^+)	4	5.068	8.8×10^{4}	2.22×10^{5}	0.103
^{168}Ir → ^{164}Re	(2^-)	(2^-)	0	6.375	2.3×10^{-1}	3.6×10^{-1}	0.11
^{168}Ir^m → ^{164}Re^m	(9^+)	(9^+)	0	6.485	2.12×10^{-1}	1.39×10^{-1}	0.11
^{170}Ir^m → ^{166}Re	(8^+)	(7^+)	2	6.265	2.25×10^{0}	2×10^{0}	0.088
^{170}Au → ^{166}Ir	(2^-)	(2^-)	0	7.175	2.64×10^{-3}	4.82×10^{-3}	0.094
^{170}Au^m → ^{166}Ir^m	(9^+)	(9^+)	0	7.285	1.48×10^{-3}	2.14×10^{-3}	0.094
^{172}Ir → ^{168}Re	(3^+)	(7^+)	4	5.985	2.2×10^{2}	1.34×10^{2}	0.071
^{172}Ir^m → ^{168}Re	(7^+)	(7^+)	0	6.125	8.7×10^{0}	4.27×10^{0}	0.071
^{174}Ir → ^{170}Re	(3^+)	(5^+)	2	5.624	1.58×10^{3}	1.34×10^{3}	0.056
^{174}Ir^m → ^{170}Re	(7^+)	(5^+)	2	5.817	1.96×10^{2}	1.81×10^{2}	0.056
^{180}Tl → ^{176}Au	$4^{(-)}$	(5^-)	2	6.715	1.82×10^{1}	6.9×10^{0}	0.022
^{186}Au → ^{182}Ir	3^-	3^+	1	4.912	8.02×10^{7}	1.73×10^{8}	0.009
^{186}Tl^m → ^{182}Au	(7^+)	(2^+)	6	6.016	4.58×10^{5}	3.5×10^{5}	0.008
				region II			
^{190}Bi → ^{186}Tl	(3^+)	(2^-)	1	6.863	8.18×10^{0}	7.6×10^{0}	0.018
^{192}Bi → ^{188}Tl	(3^+)	(2^-)	1	6.371	2.88×10^{2}	4.39×10^{2}	0.023
^{192}At → ^{188}Bi	3^+#	3^+#	0	7.700	1.15×10^{-2}	2.69×10^{-2}	0.04
^{194}Bi → ^{190}Tl	(3^+)	$2^{(-)}$	1	5.915	2.07×10^{4}	3.35×10^{4}	0.026
^{194}At → ^{190}Bi	$(4^-,5^-)$	(3^+)	1	7.462	2.53×10^{-1}	1.32×10^{-1}	0.052
^{194}At^m → ^{190}Bi^m	$(9^-,10^-)$	(10^-)	0	7.335	3.1×10^{-1}	2.9×10^{-1}	0.052
^{196}Bi → ^{192}Tl	(3^+)	(2^-)	1	5.436	2.66×10^{7}	6.67×10^{6}	0.028
^{198}At → ^{194}Bi	(3^+)	(3^+)	0	6.895	4.48×10^{0}	6.84×10^{0}	0.065
^{200}At → ^{196}Bi	(3^+)	(3^+)	0	6.596	8.31×10^{1}	9.14×10^{1}	0.063
^{200}At^m → ^{196}Bi^m	(7^+)	(7^+)	0	6.543	1.09×10^{2}	1.49×10^{2}	0.063
^{200}At^n → ^{196}Bi^n	(10^-)	(10^-)	0	6.669	7.62×10^{1}	4.7×10^{1}	0.063
^{200}Fr → ^{196}At	(3^+)	(3^+)	0	7.615	4.9×10^{-2}	6.07×10^{-2}	0.152
^{200}Fr^m → ^{196}At^m	10^-#	(10^-)	0	7.705	1.9×10^{-1}	3.08×10^{-2}	0.152
^{202}At → ^{198}Bi	$(2^+,3^+)$	$(2^+,3^+)$	0	6.353	4.97×10^{2}	9.39×10^{2}	0.055
^{202}At^m → ^{198}Bi^m	(7^+)	(7^+)	0	6.259	2.09×10^{3}	2.38×10^{3}	0.055
^{202}At^n → ^{198}Bi^n	(10^-)	(10^-)	0	6.402	4.79×10^{2}	5.83×10^{2}	0.055
^{204}At → ^{200}Bi	7^+	7^+	0	6.071	1.44×10^{4}	1.85×10^{4}	0.044
^{204}Fr → ^{200}At	(3^+)	(3^+)	0	7.170	1.82×10^{0}	1.88×10^{0}	0.133
^{204}Fr^m → ^{200}At^m	(7^+)	(7^+)	0	7.108	2.56×10^{0}	3.16×10^{0}	0.133
^{204}Fr^n → ^{200}At^n	(10^-)	(10^-)	0	7.154	1.08×10^{0}	2.16×10^{0}	0.133
^{206}At → ^{202}Bi	$(5)^+$	$5^{(+\#)}$	0	5.887	2.04×10^{5}	1.67×10^{5}	0.032
^{208}At → ^{204}Bi	6^+	6^+	0	5.751	1.07×10^{6}	1.05×10^{6}	0.021
^{208}Fr → ^{204}At	7^+	7^+	0	6.784	6.64×10^{1}	7.27×10^{1}	0.079
^{210}At → ^{206}Bi	$(5)^+$	$6^{(+)}$	2	5.631	1.67×10^{7}	1.17×10^{7}	0.012
^{210}Fr → ^{206}At	6^+	$(5)^+$	2	6.671	2.69×10^{2}	4.94×10^{2}	0.052

TABLE III. *(Continued.)*

α transition	I_i^π	I_j^π	l_{min}	Q_α(MeV)	$T^{\mathrm{exp}}_{1/2,\alpha}$(s)	$T^{\mathrm{calc3}}_{1/2,\alpha}$(s)	$P_0 P_\alpha$
^{212}Fr $\to$ ^{208}At	5^+	6^+	2	6.529	2.79×10^{3}	2.82×10^{3}	0.032
^{212}Pa $\to$ ^{208}Ac	7^+#	(3^+)	4	8.425	8×10^{-3}	8.67×10^{-3}	0.467
^{214}Ac $\to$ ^{210}Fr	5^+#	6^+	2	7.353	9.21×10^{0}	5.42×10^{0}	0.08
				region III			
^{212}Bi $\to$ ^{208}Tl	$1^{(-)}$	5^+	5	6.207	1.01×10^{4}	7.5×10^{3}	0.034
^{212}Bi^m $\to$ ^{208}Tl	$(8^-,9^-)$	5^+	3	6.454	2.24×10^{3}	1.21×10^{2}	0.034
^{212}At $\to$ ^{208}Bi	(1^-)	5^+	5	7.816	3.14×10^{-1}	8.53×10^{-2}	0.031
^{212}At^m $\to$ ^{208}Bi	9^-#	5^+	5	8.039	1.2×10^{-1}	1.81×10^{-2}	0.031
^{214}Bi $\to$ ^{210}Tl	1^-	5^+#	5	5.621	5.69×10^{6}	2.43×10^{6}	0.051
^{214}At $\to$ ^{210}Bi	1^-	1^-	0	8.987	5.58×10^{-7}	2.67×10^{-6}	0.034
^{214}At^n $\to$ ^{210}Bi^m	9^-	9^-	0	8.949	7.6×10^{-7}	3.32×10^{-6}	0.034
^{214}Fr $\to$ ^{210}At	(1^-)	$(5)^+$	5	8.589	5×10^{-3}	2.08×10^{-3}	0.04
^{214}Fr^m $\to$ ^{210}At	(8^-)	$(5)^+$	3	8.710	3.35×10^{-3}	1.92×10^{-4}	0.04
^{216}At $\to$ ^{212}Bi	$1^{(-)}$	$1^{(-)}$	0	7.950	3×10^{-4}	1.19×10^{-3}	0.044
^{216}At^m $\to$ ^{212}Bi^m	9^-#	$(8^-,9^-)$	0	7.863	1×10^{-4}	2.18×10^{-3}	0.044
^{216}Fr $\to$ ^{212}At	(1^-)	(1^-)	0	9.173	7×10^{-7}	4.17×10^{-6}	0.038
^{216}Fr^m $\to$ ^{212}At^m	(9^-)	9^-#	0	9.169	8.5×10^{-7}	4.25×10^{-6}	0.038
^{216}Ac $\to$ ^{212}Fr	(1^-)	5^+	5	9.236	4.4×10^{-4}	1.5×10^{-4}	0.057
^{216}Ac^m $\to$ ^{212}Fr	(9^-)	5^+	5	9.279	4.41×10^{-4}	1.17×10^{-4}	0.057
^{218}At $\to$ ^{214}Bi	1^-#	1^-	0	6.874	1.5×10^{0}	2.88×10^{0}	0.064
^{218}Fr $\to$ ^{214}At	1^-	1^-	0	8.013	1×10^{-3}	4.83×10^{-3}	0.041
^{218}Ac $\to$ ^{214}Fr	1^-#	(1^-)	0	9.373	1.08×10^{-6}	5.49×10^{-6}	0.045
^{220}Fr $\to$ ^{216}At	1^+	$1^{(-)}$	1	6.800	2.74×10^{1}	6.21×10^{1}	0.051
^{220}Ac $\to$ ^{216}Fr	(3^-)	(1^-)	2	8.348	2.64×10^{-2}	4.78×10^{-3}	0.041
^{220}Pa $\to$ ^{216}Ac	1^-#	(1^-)	0	9.650	7.8×10^{-7}	4.33×10^{-6}	0.059
^{222}Ac $\to$ ^{218}Fr	1^-	1^-	0	7.138	5.05×10^{0}	2.21×10^{1}	0.044
^{224}Ac $\to$ ^{220}Fr	0^-	1^+	1	6.327	1.06×10^{5}	4.09×10^{4}	0.053
^{224}Pa $\to$ ^{220}Ac	5^-#	(3^-)	2	7.694	8.44×10^{-1}	2.9×10^{0}	0.041
^{226}Ac $\to$ ^{222}Fr	$(1)^{(-\#)}$	2^-	2	5.535	1.76×10^{9}	3.38×10^{8}	0.074
^{228}Pa $\to$ ^{224}Ac	3^+	0^-	3	6.264	3.96×10^{6}	1.64×10^{6}	0.05
^{232}Np $\to$ ^{228}Pa	(4^+)	3^+	2	6.011	4.41×10^{8}	1.52×10^{8}	0.043
^{236}Np $\to$ ^{232}Pa	(6^-)	(2^-)	4	5.007	3.02×10^{15}	1.76×10^{14}	0.089
^{236}Am $\to$ ^{232}Np	(5^-)	(4^+)	1	6.255	5.4×10^{6}	6.64×10^{7}	0.033
^{238}Am $\to$ ^{234}Np	1^+	(0^+)	2	6.038	5.88×10^{9}	8.24×10^{8}	0.044
^{242}Am^m $\to$ ^{238}Np	5^-	2^+	3	5.637	9.88×10^{11}	6.94×10^{10}	0.115
^{246}Bk $\to$ ^{242}Am	$2^{(-)}$	1^-	2	6.075	1.56×10^{8}	2.12×10^{9}	0.075
^{246}Es $\to$ ^{242}Bk	4^-#	2^-#	2	7.735	4.55×10^{3}	3.79×10^{3}	0.019
^{248}Bk^m $\to$ ^{244}Am^m	$1^{(-)}$	1^+	1	5.715	8.53×10^{9}	6.47×10^{10}	0.148
^{248}Es $\to$ ^{244}Bk	2^-#	4^-#	2	7.159	6.48×10^{5}	4.28×10^{5}	0.027
^{244}Es $\to$ ^{240}Bk	–	–	0	7.935	7.4×10^{2}	5.89×10^{2}	0.015
^{246}Md $\to$ ^{242}Es	–	–	0	8.895	9.2×10^{-1}	4.68×10^{0}	0.008
^{246}Md^m $\to$ ^{242}Es	–	–	0	8.945	1.91×10^{1}	3.31×10^{0}	0.008
^{248}Md $\to$ ^{244}Es	–	–	0	8.695	3.5×10^{1}	1.65×10^{1}	0.009
^{250}Md $\to$ ^{246}Es	–	4^-#	0	8.305	7.43×10^{2}	2.24×10^{2}	0.01
^{254}Lr $\to$ ^{250}Md	–	–	0	8.815	2.38×10^{1}	5.14×10^{1}	0.005
				region IV			
^{252}Es $\to$ ^{248}Bk	(4^+)	6^+#	2	6.795	5.22×10^{7}	2.61×10^{7}	0.0146
^{254}Es^m $\to$ ^{250}Bk	2^+	2^-	1	6.699	4.42×10^{7}	5.87×10^{7}	0.0113
^{256}Md^m $\to$ ^{252}Es	(1^-)	(4^+)	3	7.895	5.02×10^{4}	1.39×10^{4}	0.0104
^{258}Md $\to$ ^{254}Es	8^-#	(7^+)	1	7.271	4.45×10^{6}	1.66×10^{6}	0.0088
^{258}Md^m $\to$ ^{254}Es^m	1^-#	2^+	1	7.189	$>2.85 \times 10^{5}$	3.07×10^{6}	0.0088
^{272}Rg $\to$ ^{268}Mt	5^+#, 6^+#	5^+#, 6^+#	0	11.195	4.5×10^{-3}	1.08×10^{-2}	0.0037
^{258}Lr $\to$ ^{254}Md	–	0^-#	0	8.905	4.32×10^{0}	1.43×10^{1}	0.009
^{258}Db $\to$ ^{254}Lr	–	–	0	9.505	7.14×10^{0}	1.52×10^{0}	0.0082
^{260}Md $\to$ ^{256}Es	–	$(1^+, 0^-)$	0	6.935	4.8×10^{7}	3.96×10^{7}	0.0079
^{260}Lr $\to$ ^{256}Md	–	7^-#	0	8.395	2.25×10^{2}	6.39×10^{2}	0.008

TABLE III. *(Continued.)*

α transition	I_i^π	I_j^π	l_{min}	Q_α(MeV)	$T_{1/2,\alpha}^{exp}$(s)	$T_{1/2,\alpha}^{calc3}$(s)	$P_0 P_\alpha$
$^{260}Db \rightarrow {}^{256}Lr$	–	–	0	9.495	1.69×10^{0}	1.67×10^{0}	0.0073
$^{260}Bh \rightarrow {}^{256}Db$	–	–	0	10.395	4.1×10^{-2}	4.24×10^{-2}	0.006
$^{262}Db \rightarrow {}^{258}Lr$	–	–	0	9.055	5.22×10^{1}	3.29×10^{1}	0.0068
$^{264}Bh \rightarrow {}^{260}Db$	–	–	0	9.965	1.24×10^{0}	5.16×10^{-1}	0.0054
$^{266}Bh \rightarrow {}^{262}Db$	–	–	0	9.425	2.5×10^{0}	1.49×10^{1}	0.0055
$^{268}Mt \rightarrow {}^{264}Bh$	5^+#	–	0	10.665	2.7×10^{-2}	4.33×10^{-2}	0.0043
$^{270}Bh \rightarrow {}^{266}Db$	–	–	0	9.065	2.28×10^{2}	1.25×10^{2}	0.0066
$^{270}Mt \rightarrow {}^{266}Bh$	–	–	0	10.175	6.3×10^{-3}	6.26×10^{-1}	0.0048
$^{272}Bh \rightarrow {}^{268}Db$	–	–	0	9.305	8.8×10^{0}	1.79×10^{1}	0.0078
$^{274}Bh \rightarrow {}^{270}Db$	–	–	0	8.925	2.04×10^{2}	1.96×10^{2}	0.0098
$^{274}Mt \rightarrow {}^{270}Bh$	–	–	0	10.505	8.5×10^{-1}	5.07×10^{-2}	0.0069
$^{274}Rg \rightarrow {}^{270}Mt$	–	–	0	11.485	2.9×10^{-2}	1.78×10^{-3}	0.0045
$^{276}Mt \rightarrow {}^{272}Bh$	–	–	0	9.995	7.3×10^{-1}	7.66×10^{-1}	0.0091
$^{276}Mt^m \rightarrow {}^{272}Bh$	–	–	0	10.135	1×10^{1}	3.23×10^{-1}	0.0091
$^{278}Mt \rightarrow {}^{274}Bh$	–	–	0	9.465	2.9×10^{1}	1.64×10^{1}	0.0124
$^{278}Rg \rightarrow {}^{274}Mt$	–	–	0	10.845	8×10^{-3}	2.61×10^{-2}	0.0079
$^{278}Ed \rightarrow {}^{274}Rg$	–	–	0	11.845	2.3×10^{-3}	1.05×10^{-3}	0.0046
$^{280}Rg \rightarrow {}^{276}Mt$	–	–	0	10.195	3.8×10^{0}	7.67×10^{-1}	0.0113
$^{282}Rg \rightarrow {}^{278}Mt$	–	–	0	9.505	1.9×10^{0}	4.26×10^{1}	0.017
$^{282}Ed \rightarrow {}^{278}Rg$	–	–	0	10.785	1.4×10^{-1}	1.22×10^{-1}	0.0096
$^{284}Ed \rightarrow {}^{280}Rg$	–	–	0	10.225	1.01×10^{0}	2.04×10^{0}	0.0152
$^{286}Ed \rightarrow {}^{282}Rg$	–	–	0	9.775	7×10^{1}	2.12×10^{1}	0.025
$^{288}Ef \rightarrow {}^{284}Ed$	–	–	0	10.635	1.9×10^{-1}	4.79×10^{-1}	0.0219
$^{290}Ef \rightarrow {}^{286}Ed$	–	–	0	10.395	6×10^{-2}	1.06×10^{0}	0.0398
$^{294}Eh \rightarrow {}^{290}Ef$	–	–	0	11.065	2.9×10^{-1}	4.67×10^{-2}	0.068

parity are unknown, $l_{min} = 0$ is taken. The last two columns present the calculation results and ratios of the calculated to experimental α decay half-lives. The larger the ratios, the larger the α preformation probabilities. The calculated half-lives $T_{1/2,\alpha}^{calc1}$ are obtained within the two-potential approach by using the isospin-dependent nuclear potential without preformation factor P_0 for different kinds of α decay, i.e., even-even, odd-A, and doubly odd nuclei. We can see that for ^{113}I and ^{115}Xe isotopes, the calculated α decay half-lives have significant deviations compared with experimental data, suggesting the α decay branching ratios may be overestimated and underestimated, respectively.

Figure 1 shows the ratios of calculated and experimental half-lives for Te, I, Xe, and Cs isotopes as a function of the neutron number, and the three kinds of α decay nuclei, i.e., even-even, odd-A, and doubly odd nuclei, are indicated by black squares, blue triangles, and red circles, respectively. It can be seen that in comparison with odd-A nuclei, the α preformation probabilities of doubly odd nuclei do not obviously reduce but abnormally increase in most cases, which is consistent with the previous study [19]. The reason for the abnormality may be the strong proton-neutron correlation resulting in disappearance of the blocking effect coming from both odd proton and neutron. Note that the main decay mode of ^{109}I is proton emission, then ^{108}I locates beyond the proton drip line [15,20]. The decrease in α preformation probability of ^{108}I may on account of the proton continuous spectrum effect.

As a successional test, we extract the α preformation probabilities P_α of doubly odd nuclei from the experimental α decay half-lives and analyze the trend by using Eq. (10), following the previous work treating the even-even and odd-A nuclei [52]. The whole α decay nuclei can be divided into four regions according to the nuclear shell (or subshell) effect, i.e., region I, $50 < Z < 82$ and $82 < N < 126$; region II, $82 < Z < 126$ and $82 < N < 126$; region III, $82 < Z < 126$ and $126 < N < 152$; region IV, $82 < Z < 126$ and $152 < N < 184$. Here the nuclear magic numbers are identical with the past work [52]. We assume that the α decay of both ground and isomeric states can be treated in a unified way, because the nuclear isomers have no clear difference with the ground states on α decay [39,40,58]. The calculations are performed in the framework of spherical shape, because angular momentum l in the centrifugal barrier [Eq. (8)] is not a good quantum number for the deformed potential [59]. According to the shell model, the spin and parity of doubly odd nuclei is determined by the coupling of both odd proton and neutron, resulting in various possible spin-parity states. Thus, the unfavored α decay (angular momentum l is nonzero) becomes common. As a convenience, the α preformation probabilities of unfavored α decay are not separated from the favored ones, and the only difference between the favored and unfavored α decay comes from the centrifugal potential barrier.

The calculated α decay half-lives $T_{1/2,\alpha}^{calc3}$, as the final results, take into account both the estimated α preformation probability P_α and preformation factor P_0. The parameters to P_α in Eq. (10) and the calculation results of α decay half-lives are listed in Tables II and III, respectively. In the top panel of Fig. 2, we show the products of estimated α preformation

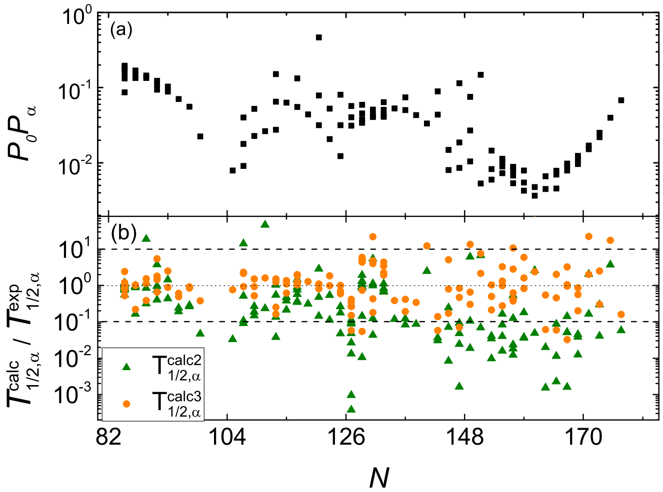

FIG. 2. (a) The products of estimated α preformation probabilities P_α and preformation factors P_0. (b) The deviations of calculated α decay half-lives, containing $T^{\rm calc2}_{1/2,\alpha}$ obtained with P_0, and $T^{\rm calc3}_{1/2,\alpha}$ obtained with both P_α and P_0.

probabilities P_α and preformation factor P_0, where the product P_0P_α presents the effective α preformation probability. In the bottom panel of Fig. 2, the deviations of both calculated α decay half-lives $T^{\rm calc2}_{1/2,\alpha}$ denoted by green triangles and $T^{\rm calc3}_{1/2,\alpha}$ indicated by yellow squares are given, respectively. Generally, as the neutron number increases, the deviations of $T^{\rm calc2}_{1/2,\alpha}$ enlarge a bit, and the α preformation probabilities become smaller. The extra neutrons can suppress the proton-neutron correlation [60], leading to little α preformation probability. We can see that the deviations of α preformation probability for heavy and superheavy nuclei ($N > 126$) are greater than those for lighter nuclei ($N < 126$). There may be two main reasons. On the one hand, deformation is common for heavy nuclei [61], and the α preformation probability for deformed nuclei is significantly different from the spherical ones [34]. On the other hand, for heavy and superheavy nuclei the single nucleon energy levels are close to the Fermi surface for both proton and neutron, and the occurrence of different subshells, e.g., $N = 152$, 162, 178, and $Z = 108$ [62–65], weaken the influence of the main shell. From Table III, we can see that the average α decay energy Q_α in region IV is large compared to the lighter mass nuclei in other regions, implying the stable limit of heavy mass nuclei.

With the above in mind, we predict the possible α decay chain beginning from the $Z = 119$ element. The predicted optimal evaporation residual cross section with ^{50}Ti + ^{249}Bk hot fusion reaction may be as large as ~10–150 fb [66,67], which nearly equals the lower limit of 30 fb. In the case of the $3n$-evaporation channel, the new doubly odd nuclide ^{296}119 can be synthesized. The α decay half-lives of nuclei from this α decay chain are calculated and listed in Table IV. Recently, ^{288}Ms and its α decay daughter nuclei have been observed in ^{48}Ca + ^{243}Am reaction [68], from which the experimental α decay energies, half-lives, and the corresponding errors are taken. The unknown α decay energies of ^{296}119 and ^{268}Db are derived from the WS4 mass model [69], which provide the most accurate prediction to reproduce the experimental Q_α values of the superheavy nuclei [70]. For ^{292}Ts, the experimental data of α decay energy and half-life are taken from the NUBASE2012 table [14]. Note that for doubly odd nuclei, α decay is the main decay mode over spontaneous fission up to the terminal nucleus ^{268}Db ($Z = 105$), resulting in the extreme long α decay chain compared with even-even nuclei [12].

For comparison, the α decay half-lives of ^{296}119 decay chain are also calculated by using various empirical formulas, i.e., semiempirical relationship based on fission (SemFIS) [71,72], universal (UNIV) curve [47,72,73], and Ni-Ren-Dong-Xu (NRDX) unified formula for α decay and cluster radioactivity [74]. The SemFIS formula, which takes into account the magic numbers at $N = 126,184$ and $Z = 82,127$ and the optimum parameters for transuranium nuclei ($Z > 92$) [72], is the best one to predict α decay half-lives [70]. From Table IV, the calculated results in this work (calc3) can well reproduce the α decay half-lives better than the UNIV and NRDX formulas. For ^{268}Db, the calculated α decay half-lives within calc3 and SemFIS are similar and comparable with the measured fission half-life, implying the competition between spontaneous fission and α decay. In addition, all the calculated α decay half-lives results of ^{296}119 and ^{292}Ts are large enough for the observation requirement (around 1 μs) [75].

IV. SUMMARY

In conclusion, we have extended the calculation of α decay for even-even and odd-A nuclei to doubly odd nuclei within the two-potential approach. For the superallowed α

TABLE IV. The α decay half-lives in the α decay chain beginning from the unknown nuclide ^{296}119.

Nucleus	Q_α (MeV)	$T^{\rm exp}_{1/2}$	$T^{\rm calc3}_{1/2,\alpha}$	$T^{\rm SemFIS}_{1/2,\alpha}$	$T^{\rm UNIV}_{1/2,\alpha}$	$T^{\rm NRDX}_{1/2,\alpha}$
^{296}119	12.449 [69]	–	150 μs	1.44 ms	2.26 ms	3.51 ms
^{292}Ts	11.285 ± 0.8	>10 ms	$28.7^{+3.2\,\rm s}_{-28.3}$ ms	$156^{+18\,\rm s}_{-154}$ ms	$263^{+28\,\rm s}_{-259}$ ms	$428^{+50\,\rm s}_{-422}$ ms
^{288}Ms	10.48 – 10.73	171^{+42}_{-28} ms	272–1232 ms	864–3958 ms	1.69–7.59 s	2.60–11.9 s
^{284}Nh	10.11(5)	$0.97^{+0.25}_{-0.17}$ s	3.07–5.82 s	6.06–11.53 s	14–26.6 s	20.1–38.2 s
^{280}Rg	9.22–10.01	$3.6^{+0.9}_{-0.6}$ s	2.45–528 s	3.17–694 s	9.0–1914 s	11.6–2526 s
^{276}Mt	9.30–10.10	$0.54^{+0.14}_{-0.09}/6^{+8}_{-2}$ s	0.4–77 s	0.37–70 s	1.28–242 s	1.47–289 s
^{272}Bh	8.86–9.29	$12.0^{+3.1}_{-2.1}$ s	20–432 s	13.6–292 s	58.6–1270 s	63.4–1373 s
^{268}Db	7.937 [69]	27^{+5}_{-4} h	38.6 h	20.3 h	117 h	108 h

decay nuclei, the α preformation probabilities of doubly odd nuclei are abnormally bigger than those of odd-A ones due to the strong correlation between the odd proton and neutron. It is also found that as the neutron number increases the α preformation probabilities show a downward trend in general, which may account for the extra neutrons. To some extent, the α preformation probabilities that extracted from the experimental α decay half-lives can be estimated by an analytic formula taking into account the shell effect and proton-neutron correlation, following our previous work. The final results can well reproduce the α decay half-lives of doubly odd nuclei. In addition, the α decay half-lives in the α decay chain beginning from the unknown doubly odd nuclide $^{296}119$ are predicted based on the above framework, and are compared with various empirical formulas. In the future, the unfavored α decay and other nuclear structure factors playing a role in α decay, e.g., the nuclear deformation, continuous spectrum, and so on, deserve further study.

ACKNOWLEDGMENTS

This work is supported by the National Natural Science Foundation of China (Grants No. 11205083 and No. 11505100), the construct program of the key discipline in Hunan province, the Research Foundation of Education Bureau of Hunan Province, China (Grant No. 15A159), the Natural Science Foundation of Hunan Province, China (Grants No. 2015JJ3103 and No. 2015JJ2121), the Innovation Group of Nuclear and Particle Physics in USC, Hunan Provincial Innovation Foundation For Postgraduate (Grant No. CX2015B398), the Shangdong Province Natural Science Foundation, China (Grant No. ZR2015AQ007).

[1] H. Geiger and J. Nuttall, Philos. Mag. **22**, 613 (1911).
[2] C. Qi, F. R. Xu, R. J. Liotta, and R. Wyss, Phys. Rev. Lett. **103**, 072501 (2009).
[3] Y. Ren and Z. Ren, Phys. Rev. C **85**, 044608 (2012).
[4] V. Viola and G. Seaborg, J. Inorg. Nucl. Chem. **28**, 741 (1966).
[5] T. Dong and Z. Ren, Eur. Phys. J. A **26**, 69 (2005).
[6] G. Gamow, Z. Phys. **51**, 204 (1928).
[7] A. B. Balantekin and N. Takigawa, Rev. Mod. Phys. **70**, 77 (1998).
[8] Y. T. Oganessian and V. K. Utyonkov, Rep. Prog. Phys. **78**, 036301 (2015).
[9] M. Pfützner, M. Karny, L. V. Grigorenko, and K. Riisager, Rev. Mod. Phys. **84**, 567 (2012).
[10] A. N. Andreyev, M. Huyse, P. Van Duppen, C. Qi, R. J. Liotta, S. Antalic, D. Ackermann, S. Franchoo, F. P. Heßberger, S. Hofmann, I. Kojouharov, B. Kindler, P. Kuusiniemi, S. R. Lesher, B. Lommel, R. Mann, K. Nishio, R. D. Page, B. Streicher, S. Saro, B. Sulignano, D. Wiseman, and R. A. Wyss, Phys. Rev. Lett. **110**, 242502 (2013).
[11] C. Qi, Rev. Phys. **1**, 77 (2016).
[12] Y. T. Oganessian, F. S. Abdullin, P. D. Bailey, D. E. Benker, M. E. Bennett, S. N. Dmitriev, J. G. Ezold, J. H. Hamilton, R. A. Henderson, M. G. Itkis, Y. V. Lobanov, A. N. Mezentsev, K. J. Moody, S. L. Nelson, A. N. Polyakov, C. E. Porter, A. V. Ramayya, F. D. Riley, J. B. Roberto, M. A. Ryabinin, K. P. Rykaczewski, R. N. Sagaidak, D. A. Shaughnessy, I. V. Shirokovsky, M. A. Stoyer, V. G. Subbotin, R. Sudowe, A. M. Sukhov, Y. S. Tsyganov, V. K. Utyonkov, A. A. Voinov, G. K. Vostokin, and P. A. Wilk, Phys. Rev. Lett. **104**, 142502 (2010).
[13] A. Sobiczewski and K. Pomorski, Prog. Part. Nucl. Phys. **58**, 292 (2007).
[14] G. Audi, M. Wang, A. Wapstra, F. Kondev, M. MacCormick, X. Xu, and B. Pfeiffer, Chin. Phys. C **36**, 1287 (2012).
[15] "NNDC at the Brookhaven National Laboratory", http://www.nndc.bnl.gov/chart/.
[16] S. N. Liddick, R. Grzywacz, C. Mazzocchi, R. D. Page, K. P. Rykaczewski, J. C. Batchelder, C. R. Bingham, I. G. Darby, G. Drafta, C. Goodin, C. J. Gross, J. H. Hamilton, A. A. Hecht, J. K. Hwang, S. Ilyushkin, D. T. Joss, A. Korgul, W. Królas, K. Lagergren, K. Li, M. N. Tantawy, J. Thomson, and J. A. Winger, Phys. Rev. Lett. **97**, 082501 (2006).
[17] S. A. Kalandarov, G. G. Adamian, N. V. Antonenko, and J. P. Wieleczko, Phys. Rev. C **93**, 054607 (2016).
[18] M. Patial, R. J. Liotta, and R. Wyss, Phys. Rev. C **93**, 054326 (2016).
[19] Y. Z. Wang, J. Z. Gu, and Z. Y. Hou, Phys. Rev. C **89**, 047301 (2014).
[20] R. D. Page, P. J. Woods, R. A. Cunningham, T. Davinson, N. J. Davis, A. N. James, K. Livingston, P. J. Sellin, and A. C. Shotter, Phys. Rev. C **49**, 3312 (1994).
[21] D. Rudolph, U. Forsberg, P. Golubev, L. G. Sarmiento, A. Yakushev, L.-L. Andersson, A. Di Nitto, C. E. Düllmann, J. M. Gates, K. E. Gregorich, C. J. Gross, F. P. Heßberger, R.-D. Herzberg, J. Khuyagbaatar, J. V. Kratz, K. Rykaczewski, M. Schädel, S. Åberg, D. Ackermann, M. Block, H. Brand, B. G. Carlsson, D. Cox, X. Derkx, K. Eberhardt, J. Even, C. Fahlander, J. Gerl, E. Jäger, B. Kindler, J. Krier, I. Kojouharov, N. Kurz, B. Lommel, A. Mistry, C. Mokry, H. Nitsche, J. P. Omtvedt, P. Papadakis, I. Ragnarsson, J. Runke, H. Schaffner, B. Schausten, P. Thörle-Pospiech, T. Torres, T. Traut, N. Trautmann, A. Türler, A. Ward, D. E. Ward, and N. Wiehl, Phys. Rev. Lett. **111**, 112502 (2013).
[22] D. N. Poenaru, *Nuclear Decay Modes* (Institute of Physics, Bristol, 1996).
[23] D. N. Poenaru, M. Ivascu, and A. Sandulescu, J. Phys. G **5**, L169 (1979).
[24] D. N. Poenaru and W. Greiner, Phys. Scr. **44**, 427 (1991).
[25] X. Bao, H. Zhang, H. Zhang, G. Royer, and J. Li, Nucl. Phys. A **921**, 85 (2014).
[26] S. Guo, X. Bao, Y. Gao, J. Li, and H. Zhang, Nucl. Phys. A **934**, 110 (2015).
[27] B. Buck, A. C. Merchant, and S. M. Perez, Phys. Rev. Lett. **65**, 2975 (1990).
[28] S. Ohkubo, Phys. Rev. Lett. **74**, 2176 (1995).
[29] D. S. Delion, A. Insolia, and R. J. Liotta, Phys. Rev. C **54**, 292 (1996).
[30] D. Ni and Z. Ren, Ann. Phys. (N.Y.) **358**, 108 (2015).
[31] Y. Qian and Z. Ren, Sci. China: Phys., Mech. Astron. **56**, 1520 (2013).
[32] D. Deng and Z. Ren, Phys. Rev. C **93**, 044326 (2016).
[33] M. Bhattacharya, S. Roy, and G. Gangopadhyay, Phys. Lett. B **665**, 182 (2008).

[34] D. S. Delion, R. J. Liotta, C. Qi, and R. Wyss, Phys. Rev. C **90**, 061303 (2014).
[35] H. F. Zhang and G. Royer, Phys. Rev. C **77**, 054318 (2008).
[36] Y. Qian and Z. Ren, Nucl. Phys. A **852**, 82 (2011).
[37] W. M. Seif, M. M. Botros, and A. I. Refaie, Phys. Rev. C **92**, 044302 (2015).
[38] M. Ismail, W. M. Seif, and A. Abdurrahman, Phys. Rev. C **94**, 024316 (2016).
[39] X.-D. Sun, P. Guo, and X.-H. Li, Phys. Rev. C **94**, 024338 (2016).
[40] X.-D. Sun, X.-J. Wu, B. Zheng, D. Xiang, P. Guo, and X.-H. Li, Chin. Phys. C **41**, 014102 (2017).
[41] R. Lovas, R. Liotta, A. Insolia, K. Varga, and D. Delion, Phys. Rep. **294**, 265 (1998).
[42] D. S. Delion, R. J. Liotta, P. Schuck, A. Astier, and M.-G. Porquet, Phys. Rev. C **85**, 064306 (2012).
[43] C. Xu, Z. Ren, G. Röpke, P. Schuck, Y. Funaki, H. Horiuchi, A. Tohsaki, T. Yamada, and B. Zhou, Phys. Rev. C **93**, 011306 (2016).
[44] D. S. Delion, R. J. Liotta, and R. Wyss, Phys. Rev. Lett. **96**, 072501 (2006).
[45] F. Xu and J. Pei, Phys. Lett. B **642**, 322 (2006).
[46] D. N. Poenaru, R. A. Gherghescu, and W. Greiner, Phys. Rev. Lett. **107**, 062503 (2011).
[47] D. N. Poenaru, R. A. Gherghescu, and W. Greiner, Phys. Rev. C **85**, 034615 (2012).
[48] Y. Qian and Z. Ren, Phys. Rev. C **94**, 064321 (2016).
[49] J. M. Wang, H. F. Zhang, and J. Q. Li, J. Phys. G **41**, 065102 (2014).
[50] X. Bao, S. Guo, H. Zhang, Y. Xing, J. Dong, and J. Li, J. Phys. G **42**, 085101 (2015).
[51] D. Poenaru, M. Ivascu, and D. Mazilu, Comput. Phys. Commun. **25**, 297 (1982).
[52] X.-D. Sun, P. Guo, and X.-H. Li, Phys. Rev. C **93**, 034316 (2016); X.-D. Sun, C. Duan, J.-G. Deng, P. Guo, and X.-H. Li, *ibid.* **95**, 014319 (2017).
[53] S. A. Gurvitz and G. Kalbermann, Phys. Rev. Lett. **59**, 262 (1987).
[54] C. Xu and Z. Ren, Nucl. Phys. A **760**, 303 (2005).
[55] B. Buck, A. C. Merchant, and S. M. Perez, Phys. Rev. C **45**, 2247 (1992).
[56] G. Royer, J. Phys. G **26**, 1149 (2000).
[57] V. Y. Denisov and A. A. Khudenko, Phys. Rev. C **79**, 054614 (2009).
[58] A. Parkhomenko and A. Sobiczewski, Acta Phys. Pol. **36**, 1363 (2005).
[59] J. Dong, W. Zuo, J. Gu, Y. Wang, and B. Peng, Phys. Rev. C **81**, 064309 (2010).
[60] U. Lombardo, P. Nozières, P. Schuck, H.-J. Schulze, and A. Sedrakian, Phys. Rev. C **64**, 064314 (2001).
[61] Z. Ren, Phys. Rev. C **65**, 051304 (2002).
[62] J. Dvorak, W. Brüchle, M. Chelnokov, R. Dressler, C. E. Düllmann, K. Eberhardt, V. Gorshkov, E. Jäger, R. Krcken, A. Kuznetsov, Y. Nagame, F. Nebel, Z. Novackova, Z. Qin, M. Schädel, B. Schausten, E. Schimpf, A. Semchenkov, P. Thörle, A. Türler, M. Wegrzecki, B. Wierczinski, A. Yakushev, and A. Yeremin, Phys. Rev. Lett. **97**, 242501 (2006).
[63] N. Wang, M. Liu, X. Wu, and J. Meng, Phys. Rev. C **93**, 014302 (2016).
[64] Y. A. Lazarev, Y. V. Lobanov, Y. T. Oganessian, V. K. Utyonkov, F. S. Abdullin, A. N. Polyakov, J. Rigol, I. V. Shirokovsky, Y. S. Tsyganov, S. Iliev, V. G. Subbotin, A. M. Sukhov, G. V. Buklanov, B. N. Gikal, V. B. Kutner, A. N. Mezentsev, K. Subotic, J. F. Wild, R. W. Lougheed, and K. J. Moody, Phys. Rev. C **54**, 620 (1996).
[65] D. Ni and Z. Ren, Nucl. Phys. A **893**, 13 (2012).
[66] V. Zagrebaev and W. Greiner, Phys. Rev. C **78**, 034610 (2008).
[67] N. Wang, J. Tian, and W. Scheid, Phys. Rev. C **84**, 061601 (2011).
[68] Y. T. Oganessian, F. S. Abdullin, S. N. Dmitriev, J. M. Gostic, J. H. Hamilton, R. A. Henderson, M. G. Itkis, K. J. Moody, A. N. Polyakov, A. V. Ramayya, J. B. Roberto, K. P. Rykaczewski, R. N. Sagaidak, D. A. Shaughnessy, I. V. Shirokovsky, M. A. Stoyer, N. J. Stoyer, V. G. Subbotin, A. M. Sukhov, Y. S. Tsyganov, V. K. Utyonkov, A. A. Voinov, and G. K. Vostokin, Phys. Rev. C **87**, 014302 (2013).
[69] N. Wang, M. Liu, X. Wu, and J. Meng, Phys. Lett. B **734**, 215 (2014); http://www.imqmd.com/mass/.
[70] Y. Z. Wang, S. J. Wang, Z. Y. Hou, and J. Z. Gu, Phys. Rev. C **92**, 064301 (2015).
[71] D. N. Poenaru, I.-H. Plonski, and W. Greiner, Phys. Rev. C **74**, 014312 (2006).
[72] D. N. Poenaru, R. A. Gherghescu, and N. Carjan, Europhys. Lett. **77**, 62001 (2007).
[73] D. N. Poenaru, R. A. Gherghescu, and W. Greiner, Phys. Rev. C **83**, 014601 (2011).
[74] D. Ni, Z. Ren, T. Dong, and C. Xu, Phys. Rev. C **78**, 044310 (2008).
[75] A. Sobiczewski, Phys. Rev. C **94**, 051302 (2016).